# Probing of Metal-Binding Domains of RNA Hairpin Loops by Laser-Induced Lanthanide(III) Luminescence†

Nancy L. Greenbaum,* Claudius Mundoma, and Dean R. Peterman‡

*Department of Chemistry, Florida State University, Tallahassee, Florida 32306-4390*

*Received September 19, 2000; Revised Manuscript Received November 30, 2000*

ABSTRACT: Direct laser excitation of aqueous Eu(III) bound to specific RNA fragments was used to probe the metal-binding sites of the anticodon loop of $tRNA^{Phe}$ from *E. coli* and of a tetraloop containing a GNRA consensus sequence. Binding of Mg(II) or Eu(III) to either RNA fragment resulted in a higher melting transition, but no global change in structure was observed. Aqueous Eu(III) exhibits a single weak excitation peak at 17273 $cm^{-1}$, the intensity of which increased upon addition of the tRNA loop fragment. Analysis of incremental increases in the luminescence intensity upon complexation with the tRNA loop indicated a stoichiometry of one high-affinity Eu(III)-binding site per loop fragment, with a $K_d$ of 1.3 ± 0.2 $\mu$M. Competition experiments between Eu(III) and Mg(II) were consistent with the two metal ions binding to a common site and with an approximately 30-fold lesser affinity of the tRNA loop for Mg(II) than for Eu(III). The rate of luminescence decay following excitation of Eu(III) bound to the tRNA loop corresponded to displacement of up to 4−5 (of a possible 9) waters of hydration on binding to the tRNA loop. By comparison, Eu(III) binds to the DNA analogue of the tRNA loop with an 8-fold lesser affinity and one fewer direct coordination site than to the RNA sequence, suggesting that a 2′OH of RNA is one of the direct ligands. In contrast with the absence of a shift in the excitation peak of aqueous Eu(III) upon formation of the tRNA loop complex, direct excitation of Eu(III) bound to a GNRA tetraloop fragment resulted in a substantially blue-shifted excitation peak (17290 $cm^{-1}$). The tetraloop fragment also has a single Eu(III)-binding site, with a $K_d$ of 12 ± 3 $\mu$M. The bound Eu(III) was competed by Mg(II), although the relative affinity for Mg(II) was approximately 150−450-fold less than that for Eu(III). The Eu(III)-binding site of the tetraloop site is highly dehydrated, with ∼7 water molecules displaced upon binding by RNA ligands, suggesting that the blue-shift of the excitation peak is the result of Eu(III) specifically bound in a nonpolar site within the GNRA loop structure.

RNA stem-loop sequences are not only a means of chain reversal within larger RNA structures but also act as nucleation sites and participate in specific tertiary interactions essential for biological function. Loop structures formed by folded RNA expose the RNA backbone and bases (*1*), creating opportunities for specific recognition by, and interaction with, protein, nucleic acid, and metal ion ligands (*2*−*4*). The loss in conformational entropy upon loop formation is partially compensated by base stacking and the formation of hydrogen bonds involving base functionalities, ribose 2′OH, or backbone nonbridging phosphate oxygen atoms (*5*). Metal ions may provide further stability by increasing the number of favorable intra- and interstrand interactions.

Cations maintain key functions in RNA structure and function through both nonspecific and specific binding (*4, 6, 7*). Formation of tertiary structure by a nucleic acid requires that negative charges of phosphates be neutralized by condensed mono- or divalent cations. The essential structural role of metals in the folding and stability of RNA molecules was revealed in the first crystallographic structures of tRNAs[1] in the 1970s, in which several tight binding sites for Mg(II) and other cations were observed (*8*−*10*), and has been further illustrated in a number of complex RNAs since then (*11*−*14*). Specifically bound divalent metal ions are also involved directly in catalysis by certain RNA motifs (*15*).

The metal-binding properties of two highly conserved and biologically important hairpin loops, the anticodon loop of $tRNA^{Phe}$ and a GAAA tetraloop, are the focus of the current investigation. Anticodon loops serve a critical function by recognizing the complementary codon sequence of mRNA, juxtaposing the aminoacylated tRNA for polymerization of amino acid to a nascent polypeptide. Binding of Mg(II) to the anticodon loop has been shown to increase its stability (*16, 17*).

The GNRA family of hairpin loops (where N is any base and R is a purine), of which the loop sequence GAAA is an example, is highly conserved in both prokaryotes and eukaryotes (*18*). The unusual stability of these four-nucleo-

† This work was partially supported by the Florida State University Council on Research and Creativity.

* Correspondence should be addressed to this author. Email: nancyg@chem.fsu.edu; Phone: (850) 644-2005; FAX: (850) 644-8281.

‡ Current address: Bechtel BWXT Idaho, P.O. Box 1625, Idaho Falls, ID 83415-5218.

[1] Abbreviations: tRNA, transfer ribonucleic acid; GNRA, an RNA stem−loop sequence of four residues, where G = guanosine, N = any base, R = any purine, and A = adenosine; MES, 2-(*N*-morpholino)-ethanesulfonic acid monohydrate; EDTA, ethylenediaminetetraacetic acid.

10.1021/bi002210u CCC: $20.00 
Published on Web 01/06/2001

tide loop structures (*19, 20*) induces pausing of reverse transcriptase catalyzed polymerization, leading to low processivity at the tetraloop hairpin region (*21*). Tetraloop hairpin motifs owe their stability to base stacking and a network of hydrogen bonds involving bases and the phosphate−sugar backbone (*20, 22*). The specific binding of metal ions may contribute further stability to these structures in situ. Evidence for specific metal ion binding sites in tetraloops comes from molecular dynamics computational studies (*23*), fluorescence (*24*), and $^{31}$P NMR spectroscopy (*25*).

Since the alkaline earth metals most commonly bound to RNA [generally Mg(II)] are spectroscopically uninformative, direct structural information about the environment of an individual bound metal ion in solution has been difficult to obtain. Distance constraints between the amino protons of cobalt hexammine, which mimics fully hydrated Mg(II) ion, and surrounding protons have been used to determine several NMR structures where RNA is bound to metal through outer sphere coordination (*26, 27*). Alternatively, the use of ions with useful spectroscopic properties permits observation of metal-binding properties of the sites (*28, 29*). For example, NMR experiments have taken advantage of the line-broadening effects of paramagnetic divalent ions, such as Mn(II) and Co(II), to obtain structural information about complexes involving RNA (*30*) and DNA (*31*). However, because of their different chemical properties, Mn(II) and Mg(II) often do not occupy the same binding site (*4*). Thus, it would be desirable to observe the putative binding of Mg(II) to RNA by replacement with a metal whose metric and chemical properties closely resemble those of Mg(II).

The metals in the lanthanide [Ln(III)] series, because of their size and chemical similarities with Mg(II) as well as their luminescence properties, are useful probes of metal-binding sites in biomolecules (*28, 32, 33*). Lanthanide metals have been shown to occupy the identical site as Mg(II) in some crystal structures of RNA (*10, 34, 35*) and readily replace Ca(II) in proteins (*36*). Emission studies with luminescent lanthanide ions bound to protein (*33, 37*), native tRNA (*38*−*40*), and the hammerhead ribozyme (*41*) have been used to probe metal-binding properties of these biomolecules. The RNA molecules studied to date involve secondary and tertiary interactions and are characterized by multiple metal-binding sites (*38*), so analyses of binding have been limited to the average behavior of the binding sites. Probing of individual binding sites would greatly enhance our understanding of the effect of metal binding on RNA structure and function.

This report details laser-induced lanthanide luminescence experiments in which Eu(III) specifically bound to small RNA fragments representing the anticodon loop of tRNA$^{Phe}$ of *E. coli*, its DNA analogue, and a GNRA tetraloop was excited directly. Quantifiable changes in luminescence intensity, excitation wavelength, and emission lifetime that occur upon Eu(III) binding to RNA, as well as metal-dependent changes in thermal stability, have been used to determine affinity and coordination properties. We show that each of the fragments has a single micromolar affinity metal-binding site for Eu(III) and that competition is observed between binding of Eu(III) and Mg(II) to both RNA fragments. From these data, we have been able to characterize binding sites of each of these highly conserved stem-loop structures in terms of coordination, binding affinity, and increase in thermal stability associated with specific binding of metal ion.

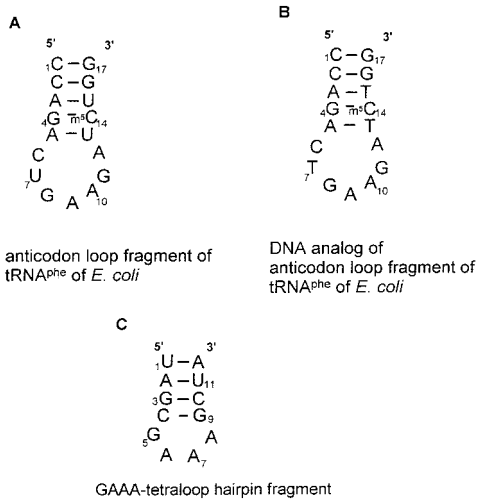


FIGURE 1: (A) Sequences and secondary structure of the yeast tRNA$^{Phe}$ anticodon stem-loop fragment and (B) its DNA analogue. The numbering scheme is specific to the fragments used in these studies. The 5-methylcytosine (m$^5$C) base at position 14 is required for Mg(II) binding by the sequence (*16*). In these experiments, the DNA analogue of the base was incorporated into the sequence (*40*). (C) Sequence for the RNA hairpin stem-loop with a GAAA tetraloop.

## MATERIALS AND METHODS

*Design and Synthesis of RNA Samples.* DNA and RNA oligomers (sequences shown in Figure 1A−C) were synthesized by standard phosphoramidite chemistry on an Applied Biosystems peptide system (ABi) converted for nucleic acid systems. Oligonucleotides were deprotected according to methods detailed in the Applied Biosystems handbook (*42*). These RNA sequences correspond to the anticodon stem-loop of yeast tRNA$^{Phe}$ (5′CCA GAC UGA AGA U$^5$mCU GG3′; Figure 1A) and its DNA analogue (Figure 1B), where $^5$mC is a methylated cytosine incorporated into the equivalent position as found in the native tRNA$^{Phe}$ sequence. The $^5$mC modification, which occurs posttranscriptionally in situ, enhances metal binding (*17*). The methylated cytosine phosphoramidite was purchased commercially as a deoxyribonucleotide (Glen Research); all other phosphoramidites were obtained from Perseptives Research. Substitution of the deoxynucleotide does not alter binding of Mg(II) in an (otherwise) RNA sequence (*43*). Although several other bases are modified in the native tRNA sequence, those modifications are not required for binding of the metal ion and have not been incorporated into samples in this study. A 12-nucleotide stem-loop sequence including a "GNRA" tetraloop sequence (5′UAGCGAAAGCUA3′) was also synthesized (Figure 1C).

Deprotected oligomers were purified by standard HPLC methods, and strand concentration was determined by the absorbance at 260 nm. RNA molecules were folded by heating to 90 °C in 10 mM MES (pH 5.0) and cooled gradually before adding 100 mM NaCl. Integrity of RNA and DNA was verified by denaturing gel electrophoresis, and the presence of a predominant (presumably the hairpin monomer) conformer was ascertained by nondenaturing gel electrophoresis.

*Eu(III) Solutions.* Stock solutions of Eu(III) were kept at a concentration of not more than 0.1 M and at a pH of between 2 and 3 to discourage base hydrolysis encountered at high concentrations and high pH. Europium was prepared by methods detailed in the literature (*44*). In brief, biological grade europium(III) oxide, $Eu_2O_3$, (Aldrich), was dissolved in redistilled concentrated perchloric acid, (99.99%) $HClO_4$, and the resulting solution was gently heated with stirring using a sand bath. Excess acid was removed by boiling the solution close to dryness, taking up the residue in water, and reducing to dryness 3 additional times. The concentration was then adjusted by dilution with doubly distilled deionized water and kept at room temperature. For luminescence measurements of Eu(III) in $D_2O$, the sample was dried down in 99% $D_2O$ twice before resuspending it in 99.96% $D_2O$ for the measurement. Eu(III) concentrations were determined by titration with standardized EDTA solution using xylenol orange as the endpoint indicator and hexamethylenetetraamine as buffer (*45*).

A typical reaction mixture for luminescence assays consisted of 30−50 $\mu$M RNA or DNA suspended in 10 mM MES, pH 5.0, and in 0.1 M NaCl (added to minimize nonspecific binding of the lanthanide to RNA). Samples were stored at 4 °C to avoid cleavage of RNA by lanthanide ions that occurs following incubation at higher temperatures (*46*). No hydrolysis of sample RNA was observed, even after the RNA had been incubated with Eu(III) for several weeks at 4 °C.

*Circular Dichroism (CD) Studies.* CD spectra were acquired on an AVIV 62DS CD system fitted with a temperature controller for the sample-handling unit. The system was interfaced to a computer with an AVIV Optics interface board. Samples were contained in a 1 mm path length quartz cell (Starna). All CD data were baseline-corrected for background signals from the cell and buffer. Each spectrum comprised the average of three scans.

*Melting Transition Studies.* Circular dichroism and UV−visible spectroscopy were used to obtain optical melting curves of RNA fragments. Melting experiments by CD for hairpin RNA samples in MES buffer were performed over a concentration range of 20−50 $\mu$M and were recorded as the change in ellipticity at 270 nm upon increase in temperature. UV−visible spectrophotometric studies of RNA were performed on a CARY 3E spectrophotometer (Varian) equipped with a temperature controller and a six-cell block sample holder. Melting curves were obtained from the change in absorbance at 260 nm as a function of temperature for RNA concentrations of 2−3 $\mu$M. Sample preparation and degassing followed established protocols (*47*). The temperature controller was ramped at a rate of 0.5 °C/min from 15 to 95 °C with data points collected at increments of 0.5 °C. Data were subjected to smoothing over 2.5 °C, and the melting temperature, $T_m$, was obtained using CARY 3.0 software.

*Luminescence Experiments.* Because of its useful spectroscopic properties, the lanthanide of choice for these experiments was trivalent europium, Eu(III). The f → f transitions of the trivalent lanthanides are forbidden, and the absorption bands are narrow and very weak, with extinction coefficients of not more than 10 $M^{-1}$ $cm^{-1}$, and emission lifetimes in the range of 0.1−1.0 ms (*48*). The weak absorption requires laser excitation in order to provide sufficient intensities for observation of the Eu(III) $^7F_0 \rightarrow {}^5D_0$ transition used in these studies. Both the ground state and the excited state are nondegenerate, which results in each distinct Eu(III) environment exhibiting a unique frequency in the excitation spectrum.

Eu(III) in solution was excited directly with a pulsed dye laser. Samples were contained in semi-micro quartz luminescence cuvettes (Starna) with internal dimensions of approximately 4 × 4 × 20 $mm^3$. Nominal volumes of 300 $\mu$L were analyzed. A fluorimeter cell adapter was used to center the cell precisely in the instrument cell compartment. The second harmonic (532 nm) of a Spectra-Physics DCR-2a 10 Hz Nd:YAG laser (9 ns pulse width, 8 mm beam waist) was used to end-pump a Spectra-Physics PDL-2 dye laser operating with an equimolar mixture of rhodamine 590 and 610 laser dyes (Exciton) in methanol. Gain wavelengths for this dye mixture were available between 575 and 600 nm with ∼0.25 $cm^{-1}$ resolution. The dye laser energy was monitored by directing a portion of the laser beam into a power meter (Laser Precision Corp. RJP-735). The sample luminescence was dispersed through a 0.25 m monochromator (Jarrel-Ash 82-410) and detected by a red-sensitive photomultiplier tube (Hamamatsu R928). Fluorescence spectra were analyzed using the deconvolution software GRAMS 386. All peaks were described by and fit to a Gaussian-Lorentzian profile.

The $^7F_0 \rightarrow {}^5D_0$ excitation spectra of Eu(III) were acquired by scanning the dye laser at the rate of 1 $cm^{-1}$/step over the 0−0 transition (17 230−17 320 $cm^{-1}$, equivalent to 580.4−577.4 nm). The sample emission from the $^5D_0 \rightarrow {}^7F_2$ hypersensitive transition was monitored at 614 nm. A LeCroy model 8013A transient digitizer TR 8828C connected through a GPIB cable to an IEEE GPIB card installed in an IBM-compatible PC was used for the collection and handling of data. Spectra were typically acquired with 50 pulses/point at 80 ns/pulse in 1.0 $cm^{-1}$ increments.

Luminescence decay lifetimes were determined by positioning the laser at the desired excitation maximum and recording the Eu(III) emission from the $^5D_0 \rightarrow {}^7F_2$ hypersensitive transition at 614 nm, and were collected on a digital storage oscilloscope (LeCroy 9410) and transferred to the computer for analysis and storage. In cases where there was no shift in the excitation spectrum of Eu(III) upon complexation with RNA, the signal attributable to partially hydrated metal (i.e., bound to RNA) was distinguished from that of fully hydrated (unbound) Eu(III) on the basis of luminescence lifetime, which increases with the number of non-$H_2O$ ligands (vide infra). For most excitation scans, we chose an acquisition gate of approximately 0.26−0.28 ms (relative to the laser trigger pulse), where the spectral contribution of unbound metal ion was much smaller than that of partially dehydrated metal (Figure 2A). Each decay curve is reported as the mean of 1000 sweeps (total acquisition time = 100 s). Curve fitting and regression analysis were performed using SigmaPlot graphics software (Jandel Scientific).

Steady-state luminescence emission spectra of Tb(III) in aqueous solution and complexed with RNA were acquired using a Spex Fluorolog II spectrofluorimeter. A 450 W high-pressure mercury/xenon lamp was used as a light source. The excitation wavelength was 280 nm, and a 308 nm cutoff filter was used to eliminate scattered light.

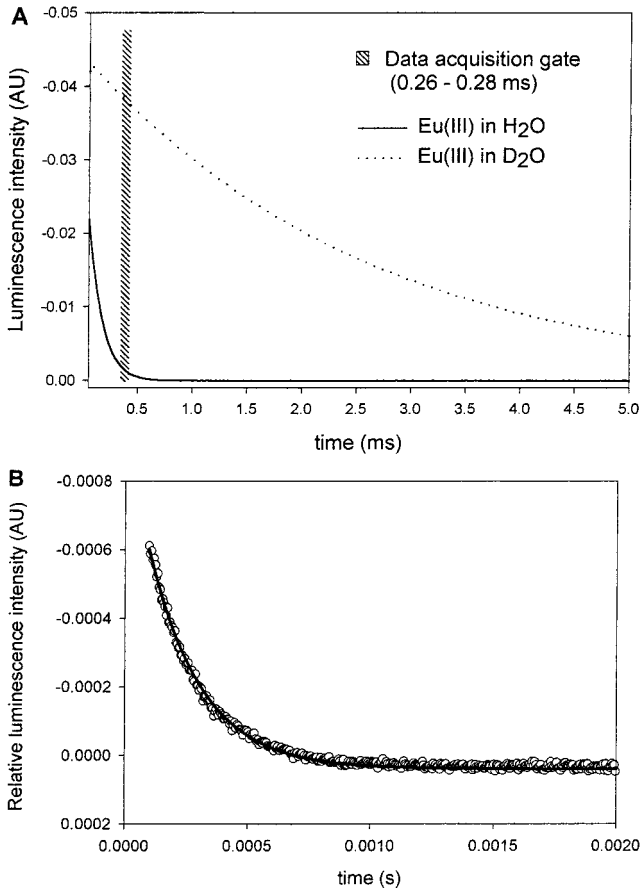


FIGURE 2: (A) Luminescence decay plots for Eu(III) in $H_2O$ (—) and in $D_2O$ (•••). The shaded region illustrates the acquisition gate at which emission data were collected for excitation spectra. This gate was chosen for most experiments in order to favor acquisition of the emission signal from partially dehydrated (i.e., bound) Eu(III) over that of fully hydrated Eu(III). (B) Representative luminescence decay plot for Eu(III) complexed with the tRNA anticodon loop fragment. Experimental details are described under Materials and Methods. The points are actual data, and the curve is the best fit single exponential ($R_2 = 0.9973$) with a decay constant, $k_{obs}$, for the Eu(III) bound to the RNA fragment of 4.480 ± 0.003 $ms^{-1}$, a value corresponding to 4.3 bound waters of hydration (eq 1). Results of luminescence lifetime measurements are summarized in Table 1.

## RESULTS

*Increased Stability of the tRNA Anticodon Loop upon Binding to Metal Ion.* The transition between an ordered, native structure and disordered, denatured state in a nucleic acid can be monitored by circular dichroism. The CD spectrum of the tRNA loop fragment was characterized by peaks and troughs typical of A-form RNA helices (*49*) and consistent with previous CD spectra of this sequence (*40*) (Figure 3). Upon the addition of equimolar concentrations of Mg(II) or Eu(III) to tRNA, there were very small changes in the 270 nm and the 190−200 nm bands (Figure 3). This observation, attributed to small alterations in base stacking and backbone conformation, is consistent with previous spectral analysis of this RNA sequence bound to Mg(II) (*43*). Only in the presence of a large excess of Mg(II) (15 mM) was a shift in the 270 nm band to shorter wavelengths observed (data not shown). Because precipitation occurs upon addition of high concentrations of Eu(III) to RNA, the CD spectrum of the tRNA anticodon loop fragment in the presence of millimolar concentrations of Eu(III) could not be obtained for comparison.

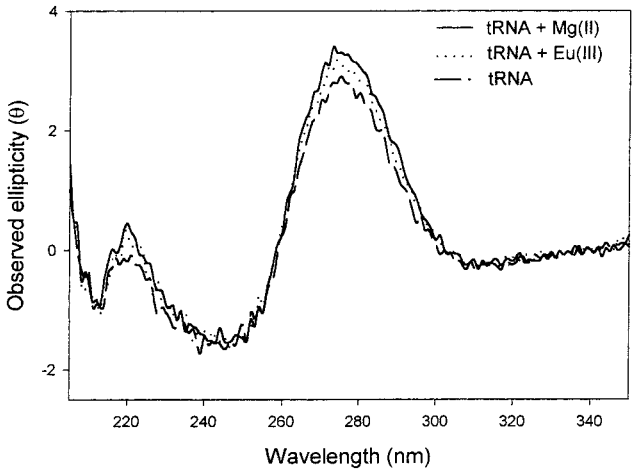


FIGURE 3: Effect of added Mg(II) and Eu(III) on the CD spectra of the anticodon loop fragment from $tRNA^{Phe}$. Circular dichroism spectra of the $tRNA^{Phe}$ anticodon loop fragment (35 μM RNA) were collected in 10 mM MES (pH 5.0) + 100 mM NaCl in the presence [50 μM Mg(II) or 38 μM Eu(III)] or absence of added metal ion at 25 °C.

The effect of bound metal ion on the stability of the folded tRNA fragment and its DNA analogue was examined by determination of the melting transition of each molecule in the presence and absence of approximately equimolar concentrations of metal ion. The melting curve for the tRNA loop in the absence of metal was sigmoidal, with a single transition observed at 45.3 °C (±0.5 °C on all measurements). In the presence of stoichiometric amounts of Mg(II), the transition became broader, with a $T_m$ of 53.8 °C. The curve recorded upon cooling the samples with and without Mg(II) from 90 to 5 °C was indistinguishable from that obtained in the forward direction. The melting curve of the tRNA anticodon loop or its DNA analogue with added Eu(III) had a broad curve with a $T_m$ of approximately 50.5 °C. The heating and cooling curves of the DNA analogue in the presence of Eu(III) were superimposable, indicating reversibility of the folding and unfolding process. The curve obtained upon cooling the RNA−Eu(III) sample, however, showed marked hysteresis. HPLC analysis of the sample following heating indicated multiple shorter products for the sample heated in the presence of Eu(III), but not for the sample incubated with Mg(II) (chromatograms not shown) This observation is consistent with the observation of Eu(III)-induced RNA cleavage at elevated temperatures reported previously by others (e.g., *28*).

Melting transitions of each fragment were also performed by measuring changes in CD at 270 nm as a function of temperature. Results were essentially the same as those measured by UV spectroscopy despite the 10-fold difference in RNA concentration between the CD (20−50 μM RNA) and the absorbance (2−3 μM RNA) measurements. The lack of dependence of the $T_m$ on concentration of RNA is consistent with a unimolecular (hairpin to coil) transition.

*Excitation Spectra.* In agreement with previous studies, direct excitation of Eu(III) in aqueous buffer resulted in a single weak luminescence excitation peak at 17 273 $cm^{-1}$ (578.9 nm), with a width at half peak height of approximately 15 $cm^{-1}$ (Figure 4A, trace a). No emission was observed in

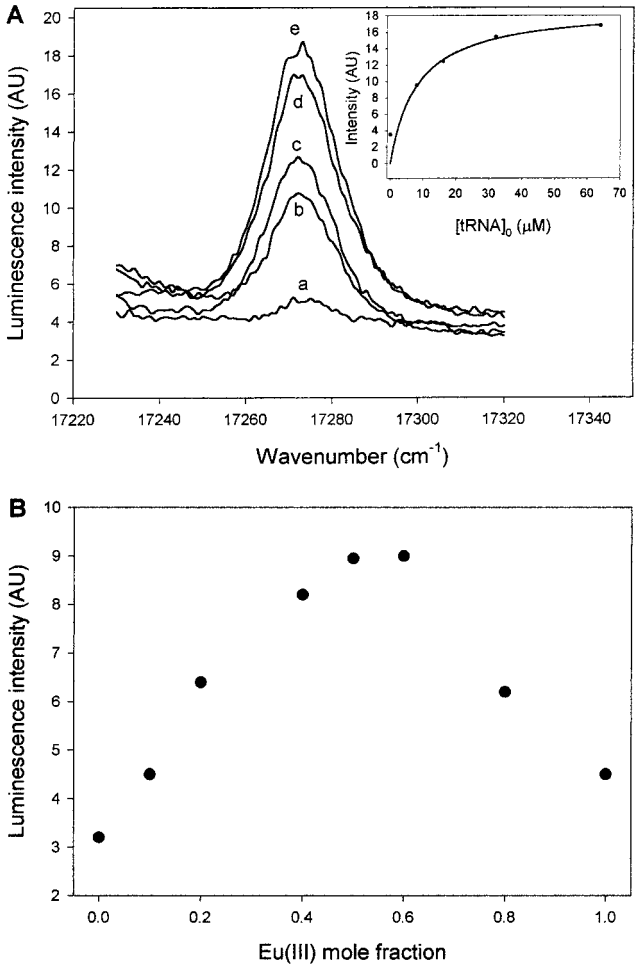


FIGURE 4: (A) Excitation spectra of Eu(III) + tRNA anticodon loop fragment. For each spectrum, [Eu(III)] = 30 $\mu$M and the concentration of tRNA was varied. [tRNA]: a = 0; b = 8 $\mu$M; c = 16 $\mu$M; d = 32 $\mu$M; and e = 64 $\mu$M. Inset: plot of the peak intensities versus the added [tRNA]. Data were fit to a standard binding isotherm (solid line) corresponding to a binding constant of 1.3 ± 0.2 $\mu$M. (B) Plot of mole fraction of Eu(III) versus luminescence intensity. Relative luminescence intensity is greatest at approximately 0.5 mole fraction of Eu(III), corresponding to one Eu(III) per RNA stem−loop fragment.

the absence of the metal. The excitation spectrum obtained after addition of tRNA loop fragment to the Eu(III) in aqueous solution exhibited an increase in intensity (Figure 4A, traces b−e). Because the wavelength of peak excitation did not change upon binding of Eu(III) to the tRNA loop and no new peaks appeared, we distinguished contributions from partially hydrated metal (i.e., bound to RNA) from fully hydrated Eu(III) to total signal by adjusting the delay and the duration of the acquisition gate to enhance the detection of the partially hydrated metal signal relative to the signal of the fully hydrated metal ion (see Materials and Methods and Figure 2A). Titration of the tRNA loop fragment into Eu(III) resulted in an incremental increase in luminescence intensity until saturation was reached at an approximately 1:1 molar ratio (Figure 4A, inset). Similar results were obtained when the titration was carried out in the reverse order; i.e., aliquots of Eu(III) were added to a constant concentration of the tRNA loop fragment. Data fit to a standard binding isotherm (Figure A, inset) resulted in a dissociation constant, $K_d$, of 1.3 ± 0.2 $\mu$M. To verify stoichiometry, both [RNA] and [Eu(III)] were varied simultaneously, and their relative mole fraction was plotted vs luminescence intensity. Maximum intensity was coincident with the optimum mole fraction of Eu(III) equal to 0.5−0.6, most consistent with a Eu(III):RNA stoichiometry of 1:1 (Figure 4B).

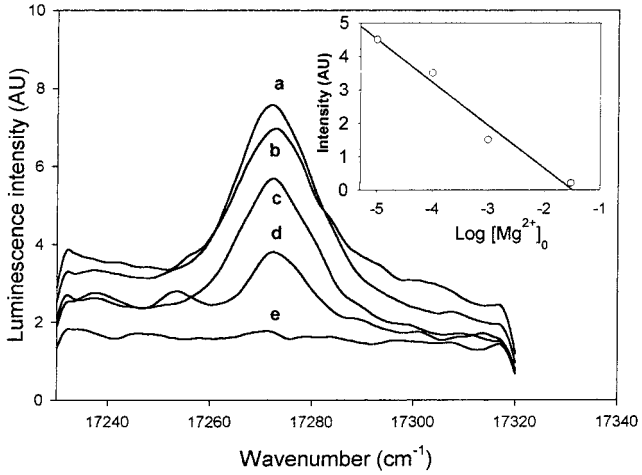


FIGURE 5: Titration of the Eu(III)−tRNA loop complex with Mg(II). a = 30 $\mu$M Eu(III) + 25 $\mu$M tRNA; b = a + 10 $\mu$M Mg(II); c = a + 100 $\mu$M Mg(II); d = a + 1 mM Mg(II); and e = a + 30 mM Mg(II). Inset: semilogarithmic plot of Mg(II) concentration vs luminescence peak intensity. Each data point was calculated as the difference between the peak maximum and the baseline of the spectrum.

Similar experiments were performed for the DNA analogue of the tRNA anticodon loop, and essentially identical results were obtained, e.g., a single excitation peak at 17 273 cm$^{-1}$ and similar saturation behavior of the signal indicating a 1:1 stoichiometry. Analysis of the binding isotherm yielded a $K_d$ of 10.0 ± 1.2 $\mu$M.

The ability of Tb(III) to bind to the tRNA anticodon loop fragment was ascertained by changes in steady-state Tb(III) luminescence after mixing with the tRNA fragment. Upon excitation at 280 nm, Tb(III) ion exhibited a fluorescence emission spectrum characterized by a small peak at 489 nm and a larger peak centered at 543 nm. Binding was monitored by an increase in the emission intensity at 543 nm. Analogous to the results obtained upon incubation of Eu(III) with the tRNA loop, luminescence of Tb(III) at each of these peaks increased upon addition of aliquots of RNA to Tb(III) or of Tb(III) to RNA, with no observable shifts in the emission spectra. Saturation of the peak at 543 nm appeared at a Tb(III):RNA ratio of approximately 1−1.5:1 (data not shown).

*Competition with Mg(II).* The question of whether Mg(II) and Eu(III) have a common binding site was addressed by competition experiments between Mg(II) and Eu(III) for the binding site. A late acquisition gate was used for data collection, thereby favoring detection of luminescence of the RNA-bound (partially dehydrated) Eu(III) and not the displaced (fully hydrated) metal. Additions of Mg(II) to a 1:1 tRNA loop/Eu(III) complex resulted in an incremental decrease in luminescence intensity (Figure 5). A semilogarithmic plot of added Mg(II) vs decrease in luminescence was linear (Figure 5, inset), consistent with Mg(II) and Eu(III) competing for the same site and the anticodon stem-loop of this tRNA having an affinity for Mg(II) approximately 30-fold less than that for Eu(III).

Table 1: Luminescence Decay Constants and Coordination Properties of the Anticodon Loop of $tRNA^{Phe}$, Its DNA Analogue, and the GAAA Tetraloop Fragments[a]

| sample | solvent | decay constant $k_{obs}$, $ms^{-1} \pm$ SD (no. of trials) | no. of coordinated $H_2O$ molecules, $Q$ ($\pm 0.5$) | direct no. of coordination to molecule, $(9 - Q) \pm 0.5$ |
|---|---|---|---|---|
| Eu(III) | $H_2O$ | $9.11 \pm 0.07$ (5) | 9.1 | |
| Eu(III) | $D_2O$ | $0.40 \pm 0.02$ (3) | − | − |
| Eu(III) + tRNA loop | $H_2O$ | $4.51 \pm 0.06$ (6) | 4.3 | 4.7 |
| Eu(III) + DNA analogue of tRNA loop | $H_2O$ | $5.55 \pm 0.07$ (5) | 5.4 | 3.6 |
| Eu(III) + GAAA loop | $H_2O$ | $1.78 \pm 0.15$ (5) | 1.4 | 7.6 |
| Eu(III) + GAAA loop | $D_2O$ | $0.57 \pm 0.03$ (2) | 0.2 | − |

[a] RNA constructs used are as in Figure 1. Samples were suspended in 10 mM MES buffer, pH 5, with 100 mM NaCl. Measurements were obtained at room temperature as outlined under Materials and Methods. For the tRNA loop−Eu(III) mixtures, the following reactant conditions were used: tRNA loop = 25 $\mu$M; DNA analogue = 25 $\mu$M; and Eu(III) = 30 $\mu$M. For the GAAA tetraloop−Eu(III) mixtures, 38.5 $\mu$M GAAA and 25 $\mu$M Eu(III) were used. The value $Q$ is defined as the number of waters of hydration coordinated to the inner sphere of Eu(III) (eq 1). All values are reported ± SD. The value in parentheses indicates the number of independent determinations.

*Coordination of Eu(III) to the tRNA Loop.* Ions interact with RNA at specific sites either by inner sphere coordination, which involves direct binding of dehydrated metal ion with specific ligands of the RNA, or by outer sphere complexes, where coordination is mediated by water molecules. The rate constant for the luminescence decay, $k_{obs}$, has previously been shown to be proportional to the number of water molecules coordinated to the inner sphere of the Eu(III) ion (*50*):

$$Q_{Ln} = A_{Ln}(k_{obs} - k_{D_2O}) \quad (1)$$

where $Q_{Ln}$ is the number of water molecules directly coordinated to the lanthanide, and $k_{obs}$ and $k_{D_2O}$ are the observed luminescence decay constants for the complex in aqueous solvent and in $D_2O$ in $ms^{-1}$, respectively. For Eu(III), the constant $A = 1.05$, and $k_{D_2O}$ was measured as $0.40 \pm 0.02$ $ms^{-1}$ (Figure 2A; data summarized in Table 1). A luminescence decay constant of $9.11 \pm 0.07$ $ms^{-1}$ was measured for Eu(III) in aqueous solution (no RNA). Substituting into eq 1, this value corresponds to 9.2 coordinated water molecules (±0.5 water molecule, the generally accepted limit of precision), a value consistent with the known coordination number of 8 or 9 for Eu(III). The luminescence following excitation of the Eu(III) bound to RNA at its peak of 17 273 $cm^{-1}$ exhibited a decay constant of $4.51 \pm 0.06$ $ms^{-1}$ (mean of triplicate determinations; Table 1; see Figure 2B for a representative decay plot). Substitution into eq 1 yielded $4.3 \pm 0.5$ waters of hydration bound to the inner sphere of the Eu(III) ion. Assuming relatively low quenching properties of RNA functional groups, up to 5 waters of hydration are replaced by inner sphere coordinations to RNA (an underestimate if there is significant quenching by nonwater ligands). By comparison, the decay constant for the Eu(III) bound to the DNA analogue of the tRNA loop was $5.55 \pm 0.07$ $ms^{-1}$. This value corresponds to $5.4 \pm 0.5$ waters of hydration in the inner sphere of the Eu(III) ion, or up to 4 inner sphere coordinated sites to DNA, i.e., one fewer direct coordination to the DNA sequence than to its RNA equivalent. Since the structures of the RNA and DNA sequences have been shown to be almost identical (*51*), the difference of one inner sphere coordination between Eu(III) bound to RNA and DNA analogues of the loop sequence suggests that a 2′OH group is involved in direct binding to the metal.

*CD Studies of a GNRA Tetraloop.* CD spectra were obtained for a stem-loop fragment containing a consensus

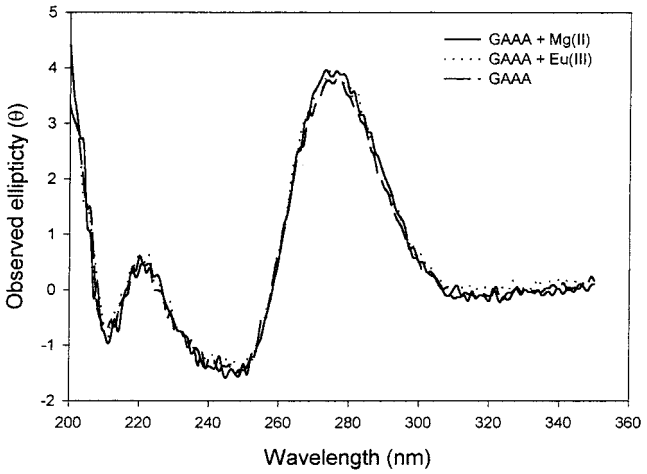


FIGURE 6: CD spectra of the GAAA tetraloop: Effect of metal ions on the conformation of the GAAA tetraloop in 10 mM MES buffer at a pH of 5.0 and 100 mM NaCl; (- - -) 35 $\mu$M GAAA tetraloop; no change was observed in the CD spectrum with addition of 50 $\mu$M Mg(II) (—) and 38 $\mu$M Eu(III) (···) to the GAAA tetraloop fragment.

"GNRA" tetraloop sequence (Figure 1C), using the same methods as were employed for the tRNA loop sequence. The CD spectrum for the tetraloop fragment had similar characteristics as those for the tRNA anticodon loop fragment described previously, e.g., well-defined peaks and troughs in positions typical of folded A-form RNA (*46*). Addition of equimolar Eu(III) or Mg(II) resulted in no visible change in the CD spectrum (Figure 6), which suggested that there was no measurable conformational change induced by the binding of low concentrations of metal ion. The melting (5−90 °C) and cooling (90−5 °C) curves obtained by monitoring the changes in CD at 270 nm were fully reversible. The melting curves obtained by changes in the UV absorption for the tetraloop were characterized by very broad transitions and a $T_m$ of approximately 56.2 °C. Such broad melting curves, seen before for short tetraloop stem-loop fragments, reflect a lack of cooperativity within the loop (*52*). Upon addition of equimolar Mg(II), there was an increase in the melting temperature to 63.9 °C, without any substantial change in the sigmoidicity of the curve. An attempt was also made to assay the melting transition of the GNRA tetraloop fragment in the presence of Eu(III). However, a nonreversible curve was obtained, suggesting that the tetraloop RNA, as in the case of the tRNA fragment, had been cleaved upon heating in the presence of Eu(III).

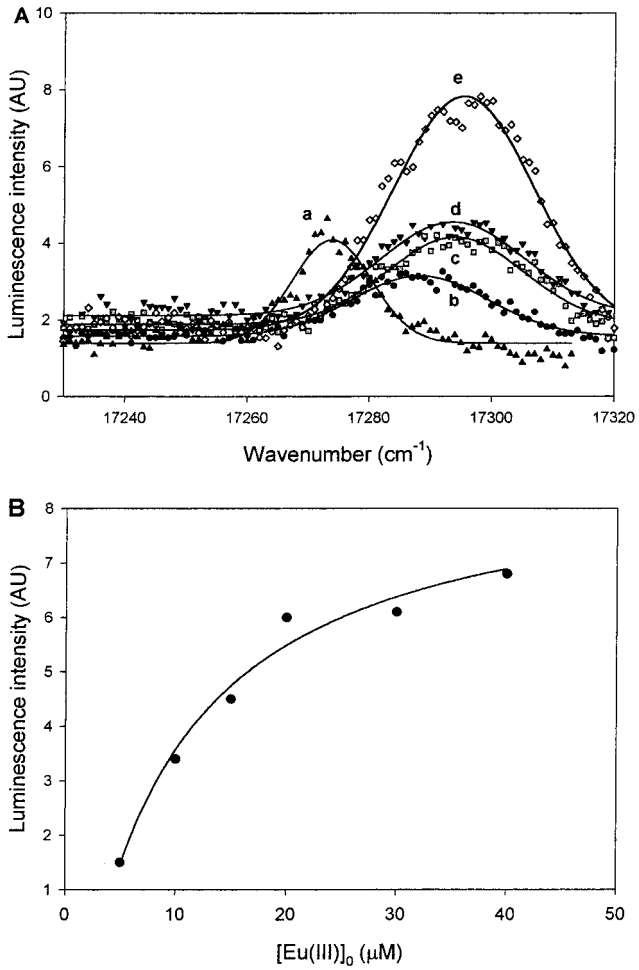


FIGURE 7: (A) Excitation spectra of the Eu(III)−GAAA tetraloop complex; spectrum a shows 5 $\mu$M Eu(III) in 10 mM MES buffer at pH 5.0 + 100 mM NaCl (no RNA). Spectra b−e were acquired from samples containing 38.5 $\mu$M GAAA tetraloop fragment (Figure 1C) incubated with the following concentrations of Eu(III): (b) 5 $\mu$M Eu(III); (c) 10 $\mu$M Eu(III); (d) 20 $\mu$M Eu(III); and (e) 40 $\mu$M Eu(III). The shift in the excitation spectra upon complexation corresponds to 17 cm$^{-1}$ (0.57 nm). Data (symbols) were fit to a Gaussian−Lorentzian profile (solid lines) to assist in visualization. (B) Plot of the luminescence intensity of the excitation peak as a function of Eu(III) concentration for data in (A). Data were fit to a standard binding isotherm with a binding constant of 12 ± 3 $\mu$M.

*Luminescence of Eu(III) Bound to the GNRA Tetraloop.* Luminescence scans and lifetimes were measured for the tetraloop fragment by the same protocol used for the tRNA anticodon loop fragment. Figure 7A shows a series of excitation spectra resulting from titration of the tetraloop RNA fragment (38.5 $\mu$M) with varied concentrations of Eu(III). The excitation spectra of Eu(III) bound to the tetraloop RNA were characterized by the appearance of a broad excitation peak centered at 17 290 cm$^{-1}$ (∼25 cm$^{-1}$ at half peak height; Figure 7A, spectra b−e), equivalent to 578.37 nm, distinct from the peak for aqueous Eu(III) at 17 273 cm$^{-1}$ (578.94 nm; Figure 7A, spectrum a). This blue-shifted excitation peak implies that the metal ion is in a distinctly different environment from that seen in aqueous solution or upon binding to other RNA molecules [this work; (*38*−*40*)]. When carried out in the reverse order, i.e., metal added to RNA, only the 17 290 cm$^{-1}$ peak was visible until a [Eu(III)]:[RNA] ratio exceeding 1:1 was achieved, after which the peak attributable to aqueous Eu(III) at 17 273 cm$^{-1}$ became visible. A plot of varying mole ratios of [RNA]:[Eu(III)] vs luminescence intensity was best fit by a stoichiometry of one metal ion per loop fragment (data not shown). A least-squares fit to the binding isotherm (Figure 7B) resulted in a dissociation constant, $K_d$, of 12 ± 3 $\mu$M. These data indicate that Eu(III) binds with moderate affinity to a single site of the tetraloop sequence.

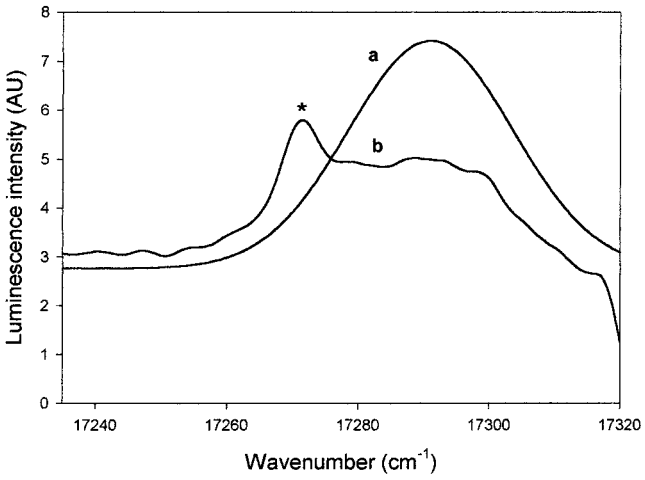


FIGURE 8: Excitation spectra of the Eu(III)−GAAA tetraloop complex [30 $\mu$M Eu(III) + 38.5 $\mu$M RNA] in the absence of Mg(II) (spectrum a) and in the presence of 15 mM Mg(II) (spectrum b). The sample was suspended in 10 mM MES buffer (pH 5.0) with 100 mM NaCl. The narrow peak (*) in spectrum b is attributed to fully hydrated Eu(III).

*Mg(II) Competition Experiments.* Mg(II) competition experiments were carried out for the tetraloop loop fragment in order to establish whether Eu(III) and Mg(II) compete for the same site. Mg(II) competition experiments were performed under two sets of starting conditions: at [Eu(III)] ≫ [RNA], so that both the peaks at 17 290 and 17 273 cm$^{-1}$ were represented in the spectrum, and at [RNA] > [Eu(III)], so that only the peak at 17 290 cm$^{-1}$ was present in the excitation spectrum. Figure 8 displays representative spectra obtained when Mg(II) was titrated into a mixture in which Eu(III) was present in excess of the tetraloop RNA fragment. Data were obtained at a sufficiently early data acquisition gate to observe contributions of both aqueous and bound Eu(III). Addition of Mg(II) resulted in the diminution of the blue-shifted peak; the small increase in luminescence intensity at 17 273 cm$^{-1}$ at high Mg(II) concentrations was attributed to a greater concentration of unbound Eu(III) upon displacement from its binding site by Mg(II). A semilogarithmic plot of added Mg(II) vs luminescence intensity at 17 290 cm$^{-1}$ indicated a 50% decrease in Eu(III) luminescence upon addition of approximately 10 mM Mg(II), consistent with a 150−450-fold lesser affinity by the tetraloop RNA for Mg(II) than for Eu(III).

*Coordination Number of Metal Binding to the GAAA Tetraloop.* The rate constant for the decay of Eu(III) luminescence at each of the two peaks following direct excitation was investigated in order to determine the number of water molecules coordinated to Eu(III) in each environment (data summarized in Table 1). Data were all fit to a single-exponential regression analysis, and the fit was excellent ($R^2 \geq 0.99$). Observed rate constants were then substituted into eq 1. Excitation of the peak at 17 290 cm$^{-1}$ resulted in luminescence with a decay constant of 1.78 ±

0.15 $ms^{-1}$, corresponding to 1.4 ± 0.5 bound water molecules (i.e., approximately 7 waters of hydration displaced on complexation with RNA). By comparison, decay of the luminescence of Eu(III) complexed to the tetraloop RNA fragment in deuterated buffer (following several exchange steps in $D_2O$ to minimize residual $H_2O$) was 0.57 $ms^{-1}$ (vs 0.40 $ms^{-1}$ in $D_2O$ alone). This value is equivalent to the displacement of 0.2 waters of hydration (eq 1), placing an upper limit on the bulk contribution of RNA ligands to quenching in this system. When there was minimal overlap between the two peaks (i.e., at a large excess of metal ion), the peak at 17 273 $cm^{-1}$ had a lifetime consistent with full hydration of the Eu(III). Alternatively, when there was substantial overlap between the peaks at 17 273 and 17 290 $cm^{-1}$ [which occurred in the presence of only a small excess of Eu(III)], a double exponent fit for the peak at 17 273 $cm^{-1}$ resolved a very short-lived signal (decay constant of 8.03 ± 0.42 $ms^{-1}$, equivalent to 8.0 ± 0.5 bound water molecules) and a long-lived component (decay constant of 1.64 ± 0.04 $ms^{-1}$, corresponding to 1.3 ± 0.5 bound water molecules).

## DISCUSSION

To examine properties of metal coordination by RNA hairpin loops, we have exploited the changes in luminescence lifetime, intensity, and excitation wavelength of lanthanide ions that occur upon specific binding to RNA. Our approach has a solid basis in small organic molecule literature, where it has provided specific information about individual binding sites (*53*, *54*). Eu(III) possesses a characteristic fluorescence spectrum in the red, with its strongest lines around 580, 593, 614, 650, and 700 nm corresponding to $^5D_0 \rightarrow {}^7F_J$ transitions, with $J = 0-4$, respectively. Both the ground state and the excited state are nondegenerate, so each distinct Eu(III) environment exhibits a singlet peak in the excitation spectrum. The $^5D_0 \rightarrow {}^7F_2$ transition at 614 nm is hypersensitive, a useful property for these spectroscopic studies because emission is enhanced for the metal−ligand complex relative to that of unbound metal ion in aqueous solution. For gaseous Eu(III), the excitation maximum has been calculated to be at 17 374 $cm^{-1}$ (575.57 nm) (*55*), whereas aqueous Eu(III) has an excitation peak that is red-shifted by 100 $cm^{-1}$ (centered at 17 273 $cm^{-1}$, or 578.94 nm).

Only trace amounts of lanthanides are known to exist in living systems, and there is no biological role attributed to them. However, chemical and metric similarities between lanthanides and Ca(II) (*28*) have enabled replacement of specific Ca(II)-binding sites in proteins with lanthanide ions (*33*, *48*). This feature has provided a successful avenue for investigation of metal-binding sites in proteins by luminescence and paramagnetic NMR techniques (*36*). The chemical and metric properties are not as close between Eu(III) and Mg(II); it is, therefore, an interesting feature of folded RNA molecules that substitution of lanthanides for Mg(II) ions is sometimes tolerated, particularly when the proximity to phosphate oxygen atoms is sufficiently close to form a cage around the ion.

Lanthanide ions will substitute for Mg(II) in some, but not all, RNA metal-binding sites. For example, crystallographic studies of $tRNA^{Phe}$ have shown that Sm(III) binds identically to Mg(II) ion in certain sites (*10*, *34*). Tb(III) binds to the hammerhead ribozyme in a site near, but not identical to, the binding site of Mg(II) (*41*). Crystallographic analysis of the Group I intron in which Mg(II) was replaced by Sm(III), however, indicated that substitution of the lanthanide perturbed the native structure (*11*, *56*). Therefore, while lanthanide ions will substitute for Mg(II) in some RNA-binding sites, this is not always the case.

Replacement of native ions with lanthanide ions has proven useful in solution studies of tRNA molecules in which the environment-specific luminescence characteristics of lanthanide ions were probed. Kayne and Cohn (*38*) and Wolfson and Kearns (*39*) monitored Eu(III) emission sensitized by 4-thiouracil, a modified base present at the junction between the acceptor stem and the D loop of particular tRNAs extracted from *E. coli*, to demonstrate the presence of several tight metal-binding sites in the vicinity. Draper used a similar method to measure the affinities of three distinct metal-binding sites in $tRNA^{Phe}$ from *E. coli* (*40*), and showed that the metal in the highest affinity site had several ligands bound directly to its inner coordination sphere. In these experiments, we have focused on metal-binding properties of a single site in a synthetic molecule by exciting the lanthanide metal ion Eu(III) directly.

*Eu(III)-Binding Properties of the Anticodon Loop of $tRNA^{Phe}$.* The anticodon loop of a tRNA molecule presents anticodon imino, amino, and carbonyl groups to complementary groups of mRNA in an environment sufficiently structured to facilitate efficient pairing with minimal loss of conformational entropy. Stability of the loop structure is enhanced by the specific binding of metal ions, the affinity for which is increased by the presence of posttranscriptionally modified bases, including methylated bases and pseudouridines (*57*, *58*). The importance of thermal stability is underscored by the observation that tRNAs of cultured thermophilic bacteria exhibit an increased level of base modification when grown at elevated temperatures (*59*).

Consistent with the work of Agris and colleagues on the binding of a tRNA anticodon loop or its DNA analogue to Mg(II) (*43*), we observed a small increase in ellipticity at 270 nm upon incubation with stoichiometric amounts of either metal ion. These spectral changes suggest a slight conformational change resulting from base stacking and backbone alterations upon binding. Only upon the addition of millimolar quantities of Mg(II) was a large spectral change observed (*43*), making it unlikely that these changes are attributable to high-affinity binding. The melting transition of the DNA analogue of the tRNA anticodon loop displayed an increase in $T_m$ upon addition of Mg(II) or Eu(III) [not measured for the tRNA loop because of Eu(III)-induced cleavage upon heating].

Changes in the luminescence intensity and the lifetime of Eu(III) upon binding to the tRNA loop fragment or its DNA analogue demonstrated that specific, moderately high-affinity (1.3 and 10 $\mu$M, respectively) binding took place. There was no change in the wavelength of maximal excitation of the metal when bound to the tRNA sequence; this was also the case in the previous luminescence studies of whole tRNA (*40*) and the hammerhead ribozyme sequence (*41*). As with Eu(III), the luminescence of Tb(III) increased upon addition of the tRNA anticodon loop fragment. However, with Eu(III), and not with Tb(III), the ground state is nondegenerate, and so a given peak represents a unique coordination environment (*48*). Furthermore, excitation at 280 nm involves

a complex sum of direct excitation of the Tb(III) and energy transfer from the surrounding RNA "antenna". For these reasons, subsequent experiments were carried out using Eu(III). Nonetheless, it was useful to demonstrate that the Ln(III)-binding properties of this RNA fragment are not limited to Eu(III).

The stoichiometry of binding, measured from the relative intensity of the emission signal at varied RNA:Eu(III) ratios, was most consistent with one high-affinity binding site for Eu(III) per tRNA stem-loop fragment. This value contrasts with the calculation of two Mg(II) ions bound to the same sequence, based upon values derived from CD data by Agris and co-workers (*43*). Only a single Mg(II)-binding site was noted in crystal structures of the anticodon loops of various tRNAs (*10, 34, 60*). However, a spermine-binding site was also observed in the stem that could represent a low-affinity Mg(II)-binding site in solution (*61*). The binding algorithm used by Agris and colleagues (*43*) yielded a composite dissociation constant for the two ions, from which it was not possible to differentiate the relative affinity for each. From our competition data between Mg(II) and Eu(III), a $K_d$ for Mg(II) of approximately 40 $\mu$M can be inferred. Because of precipitation at high [Eu(III)], we were not able to obtain reliable data beyond a 2-fold excess of Eu(III). Therefore, although we could not assay for a low-affinity site, it is plausible that the binding site we observed corresponds to the higher affinity site of the two predicted by Agris and colleagues.

Our coordination experiments on the tRNA anticodon loop have indicated that there are 4 waters of hydration ($\pm$0.5, the limit of accuracy) coordinated to the inner sphere of the lanthanide ion. The nonintegral number of coordinated water molecules may be attributed to the presence of species with different extents of hydration in dynamic equilibrium or to quenching by nonwater ligands, neither of which can be distinguished using the current data. From the number of water molecules bound to the RNA, and assuming a coordination number of up to 9 ligands, the tRNA anticodon loop may have up to 5 direct coordinations to the metal. Since Eu(III) is a "hard" acid, similar to Mg(II), it will share preferences for "hard" base ligands, e.g., keto oxygen, 2′OH, or phosphate oxygen. Crystal structures of the $tRNA^{Phe}$ anticodon loop have shown one inner sphere coordination between Mg(II) and a backbone phosphate group, with the others being water-mediated hydrogen bonds to bases. Jack et al. (*10*) reported that lanthanides such as Sm(III) coordinate highly to oxygen in a distorted octahedral geometry (i.e., six strongly bound ligands), plus three coordination positions are occupied by the solvent, usually water molecules. If the binding site for Mg(II) and Eu(III) is the same, as our competition data suggest for this molecule, the greater number of inner sphere coordinations seen here for the binding of Eu(III) implies that each of the additional coordination sites are direct, coordinations for which we might anticipate a substantially greater affinity. For example, the difference in affinity of an EDTA−Mg(II) complex vs EDTA−Eu(III) complex is approximately 3 orders of magnitude (*62*). By comparison, the Eu(III)−tRNA loop complex has an affinity only 30 times greater than that of the tRNA loop with Mg(II). This observation suggests to us that the binding of the slightly larger ion may induce some distortion in the binding site to make its binding less favorable than would be predicted by an incremental increase of three direct coordinations.

We tested the possibility that one or more of the inner sphere coordinations involves a 2′OH group by measuring the luminescence lifetime of Eu(III) bound to the DNA analogue of the anticodon loop. Our results indicated that there was one fewer direct coordination for the DNA fragment than for the RNA analogue, and the affinity of the DNA analogue for Eu(III) was somewhat lower than that of the RNA ($K_d$ of 1.3 $\mu$M vs 10 $\mu$M for RNA and DNA, respectively). The solution structure of the DNA analogue of the $tRNA^{Phe}$ anticodon loop determined by Basti et al. (*51*) demonstrated the strong structural similarity of RNA and DNA fragments. The most plausible explanation for the difference in coordination number by an integer, and the relative difference in affinity between Eu(III) bound to the DNA and RNA analogues, is that one of the coordinations in the RNA sequence involves a 2′OH group. A 2′OH was not observed, however, as a direct ligand to Mg(II) in the tRNA crystal structure (*10, 34*). Whether this interaction with the 2′OH is specific to coordination with Eu(III) or is due to differences in the interaction between crystal and solution structures is not currently clear.

*Eu(III)-Binding Properties of an RNA Tetraloop.* To elucidate the characteristics of metal binding to biologically significant RNA structural elements, we applied similar methods to examine the metal-binding properties of a GNRA tetraloop, an RNA sequence often studied because of its unusual stability. Solution structures of two of the most common tetraloop motifs, those with UNCG and GNRA loop sequences, elucidated the structural basis for the observed stability (*63*).

The complete absence of change in the CD spectrum following incubation of the GNRA sequence with Mg(II) or Eu(III) suggests that no measurable change occurs in base stacking and backbone conformation in the presence of either metal ion. Substantial changes in the luminescence lifetime and a significant blue-shift in the excitation peak [with respect to the peak of Eu(III) in aqueous solution] were observed, confirming that binding of Eu(III) to the tetraloop fragment indeed occurred. This conclusion was further supported by specific information about binding stoichiometry and affinity derived from changes in peak intensity and luminescence lifetime upon addition of metal ion. Because of the shift in peak excitation, we were able to quantify a change in the formation of the RNA−metal complex from the intensity of the new peak alone. A Eu(III):RNA stoichiometry of 1:1 was observed for this complex, and the affinity for Eu(III) was 12 $\pm$ 3 $\mu$M. Mg(II) competed with Eu(III) for binding, with 150−450-fold excess of Mg(II) required to decrease the Eu(III) luminescence by 50%. Two models could explain the competition data: (1) Mg(II) and Eu(III) compete for the identical site, but Eu(III) binds with substantially greater affinity than does Mg(II); or (2) the two metals bind at independent sites, but binding of Mg(II) induces a conformational change that perturbs the nearby Eu(III)-binding site. If the affinity for Mg(II) is in the millimolar range, it would be difficult to explain the increase in the melting transition of 7 °C we observed upon addition of equimolar amounts of the ion (since only ~10% of it would be bound). We therefore favor the interpretation that Mg(II) and Eu(III) bind to nearby, but not identical, sites. A

similar geometry was observed for the binding of Tb(III) and Mg(II) in the hammerhead ribozyme (*35, 41*).

We found the binding site to be highly dehydrated, with at most two water molecules bound to Eu(III). From their NMR model of the tetraloop−$Co(NH_3)_6^{3+}$ complex, Rudisser and Tinoco (*27*) observed two phosphate groups forming close contacts with the $Co(NH_3)_6^{3+}$, from which they concluded that the relatively stronger affinity for Mg(II) in the loop was a result of dehydration upon binding to the loop. The observed preference (by 3.5-fold) for binding of Mg(II) over $Co(NH_3)_6^{3+}$ by the loop (*27*) provided further evidence for dehydration of the metal ion upon binding to the tetraloop region. Results of site mutations in studies of Mn(II) binding to a similar GAAA sequence have shown that nonbridging phosphate oxygen atoms are important ligands for metal binding (*25, 64*). Since Mn(II) prefers different ligands than Mg(II), however, there may be differences in the binding sites of Mg(II) or Eu(III) and those of Mn(II) (*65*).

The blue-shifted excitation peak displayed by Eu(III) upon complexation with the GAAA tetraloop appears to be novel; its observation is in contrast with excitation peaks of Eu(III) bound to the tRNA anticodon loop (this work) or the hammerhead ribozyme (*41*), which exhibit no change in excitation maximum, or excitation peaks for organic ligands, which display red-shifts correlated (to some extent) with chemical properties of the ligand (*53, 54, 66*). Catalán et al. (*67*) have correlated red- and blue-shifts in the excitation peaks of fluorophores with the polarity of intramolecular hydrogen bonds in small organic systems. Perhaps the observed spectral shift in this RNA−metal complex is the result of binding of the metal ion in a nonpolar "cage", thereby resulting in a lesser red-shift from the calculated value in a vacuum (*52*) than is seen in aqueous solvent or bound to other RNA molecules studied to date (*36*−*39*). However, its origin in this tetraloop−metal complex is not clear, and will be addressed in a separate study.

In each of the RNA−Eu(III) complexes studied, little or no structural change occurs upon coordination with the metal ion, a feature that may implicate nonspecific or diffuse binding (*6, 68*). Moreover, a relatively high affinity of binding is not necessarily associated with specificity, as condensed ions can also have a high affinity for the ligand. We would argue, however, that the metal binding exhibited by each of these RNA stem−loops is specific. In the case of the tRNA anticodon loop, there is an integral difference in the number of coordinations upon substitution of deoxyriboses for riboses, accompanied by a decrease in affinity. Likewise, the tetraloop sequence appears to provide a highly dehydrated, nonpolar environment for the metal. Further information concerning the specificity awaits additional mutation studies and determination of high-resolution structures of the RNA−metal complexes.

## ACKNOWLEDGMENT

We thank Meredith Newby for making synthetic RNA, Janice Dodge and Elizabeth Arledge for technical assistance, Prof. Gregory Choppin and Dr. Sergei Sinkov for helpful discussions, Dr. Lambertus J. van de Burgt and Dr. David Gormin of the FSU Chemistry Department Laser Laboratory, and the Biochemical Analysis Synthesis & Sequencing Laboratory.

## REFERENCES

1. Hermann, T., and Patel, D. J. (2000) *Structure 8*, R47−R54.
2. Draper, D. E. (1999) *J. Mol. Biol. 293*, 255−270.
3. Hermann, T., and Patel, D. J. (1999) *J. Mol. Biol. 294*, 829−849.
4. Pan, T., Long, D. M., and Uhlenbeck, O. C. (1993) in *The RNA World* (Gesteland, R. F., and Atkins, J. F., Eds.) pp 271−302, Cold Spring Harbor Laboratory Press, Cold Spring Harbor, NY.
5. Tinoco, I., Jr., and Bustamente, C. (1999) *J. Mol. Biol. 293*, 271−281.
6. Misra, V. K., and Draper, D. E. (1998) *Biopolymers 48*, 113−135.
7. Feig, A. L., and Uhlenbeck, O. C. (1999) in *The RNA World* (Gesteland, R. F., Cech, T. R., and Atkins, J. F., Eds.) pp 287−319, Cold Spring Harbor Laboratory Press, Cold Spring Harbor, NY.
8. Kim, S. H., Suddath, F. L., Quigley, G. J., McPherson, A., Sussman, J. L., Wang, A. H. J., Seeman, N. C., and Rich, A. (1974) *Science 185*, 435−440.
9. Robertus, J. D., Ladner, J. E., Finch, J. T., Rhodes, D., Brown, R. S., Clark, B. F. C., and Klug, A. (1974) *Nature (London) 250*, 546−551.
10. Jack, A., Ladner, J. E., Rhodes, D., Brown, R. S., and Klug, A. (1976) *J. Mol. Biol. 111*, 315−328.
11. Cate, J. H., Gooding, A. R., Podell, E., Zhou, K., Golden, B. L., Kundrot, C. E., Cech, T. R., and Doudna, J. A. (1996) *Science 273*, 1678−1685.
12. Pley, H. W., Flaherty, K. M., and McKay, D. B. (1994) *Nature 372*, 68−74.
13. Blyn, L. B., Risen, L. M., Griffey, R. H., and Draper, D. E. (2000) *Nucleic Acids Res. 28*, 1778−1784.
14. Scott, W. G., Murray, J. B., Arnold, J. R. P., Stoddard, B. L., and Klug, A. (1996) *Science 274*, 2065−2069.
15. Pyle, A. M. (1993) *Science 261*, 709−714.
16. Laing, L. G., Gluick, T. C., and Draper, D. E. (1994) *J. Mol. Biol. 237*, 577−587.
17. Chen, Y., Sierzputowska-Gracz, H., Guenther, R., Everett, K., and Agris, P. F. (1993) *Biochemistry 32*, 10249−10253.
18. Woese, C. R., Gutell, R. R., Gupta, R., and Noller, H. F. (1983) *Microbiol. Rev. 47*, 621−624.
19. Antao, V. P., Lai, S. Y., and Tinoco, I., Jr. (1991) *Nucleic Acids Res. 19*, 5901−5905.
20. Cheong, C., Varani, G., and Tinoco, I., Jr. (1990) *Nature 346*, 680−682.
21. Pop, M. P., and Biebricher, C. K. (1996) *Biochemistry 35*, 5054−5062.
22. Heus, H. A., and Pardi, A. (1991) *Science 253*, 191−194.
23. Hermann, T., and Westhof, E. (1998) *Structure 6*, 1303−1314.
24. Menger, M., Eckstein, F., and Porschke, D. (2000) *Biochemistry 39*, 4500−4507.
25. Horton, T. E., Maderia, M., and DeRose, V. J. (2000) *Biochemistry 39*, 8201−8207.
26. Kieft, J. S., and Tinoco, I., Jr. (1997) *Structure 5*, 713−721.
27. Rudisser, S., and Tinoco, I., Jr. (2000) *J. Mol. Biol. 295*, 1211−1223.
28. Evans, C. H. (1990) *Biochemistry of the Lanthanides*, Plenum Press, New York.
29. McNemar, C. W., and Horrocks, W. D., Jr. (1990) *Biochim. Biophys. Acta 1040*, 229−236.
30. Allain, F. H.-T., and Varani, G. (1995) *Nucleic Acids Res. 23*, 341−350.
31. Gochin, M. (1998) *J. Am. Chem. Soc. 119*, 3377−3382.
32. Horrocks, W. D., Jr., and Sudnick, D. R. (1981) *Acc. Chem. Res. 14*, 384−392.
33. Horrocks, W. D., Jr. (1993) in *Methods in Enzymology*, pp 495−538, Academic Press, San Diego.
34. Stout, C. D., Mizuno, H., Rao, S. T., Swaminathan, P., Rubin, J., Brennan, T., and Sundaralingam, M. (1978) *Acta Crystallogr. B34*, 1529−1544.

35. Feig, A. L., Scott, W. G., and Uhlenbeck, O. C. (1998) *Science 279*, 81−84.
36. Lee, L., and Sykes, B. D. (1983) *Biochemistry 22*, 4366−4373.
37. Bruno, J., Horrocks, W. D., Jr., and Zauhar, R. J. (1992) *Biochemistry 31*, 7016−7026.
38. Kayne, M. S., and Cohn, M. (1974) *Biochemistry 13*, 4159−4165.
39. Wolfson, J. M., and Kearns, D. R. (1975) *Biochemistry 14*, 1436−1444.
40. Draper, D. E. (1985) *Biophys. Chem. 21*, 91−101.
41. Feig, A. L., Panek, M., Horrocks, W. D., Jr., and Uhlenbeck, O. C. (1999) *Chem. Biol. 6*, 801−810.
42. *Evaluation and Purification of Synthetic Oligonucleotides*, Applied Biosystems User Bulletin, Revised [13], 1987.
43. Dao, V., Guenther, R. H., and Agris, P. F. (1992) *Biochemistry 31*, 11012−11019.
44. Bünzli, J.-C. G., Moret, E., and Yersin, J.-R. (1978) *Helv. Chim. Acta 61*, 762−771.
45. Fritz, J. S., Oliver, R. T., and Piertrzyk, D. J. (1958) *Anal. Chem. 30*, 1111−1114.
46. Geyer, C. R., and Sen, D. (1998) *J. Mol. Biol. 275*, 483−489.
47. Puglisi, J. D., and Tinoco, I., Jr. (1989) in *Methods in Enzymology*, pp 304−324, Academic Press, Inc., San Diego.
48. Horrocks, W. D., Jr., and Albin, M. (1984) in *Progress in Inorganic Chemistry* (Lippard, S. J., Ed.) pp 1−104, John Wiley & Sons, New York.
49. Johnson, W. C., Jr. (1996) in *Circular Dichroism and the Conformational Analysis of Biomolecules* (Fasman, G. D., Ed.) pp 433−468, Plenum Press, New York.
50. Horrocks, W. D., Jr., and Sudnick, D. R. (1979) *J. Am. Chem. Soc. 101*, 334−340.
51. Basti, M. M., Stuart, J. W., Lam, A. T., Guenther, R., and Agris, P. F. (1996) *Nat. Struct. Biol. 3*, 38−44.
52. Worner, K., Strube, T., and Engels, J. W. (1999) *Helv. Chim. Acta 82*, 2094−2014.
53. Albin, M., and Horrocks, W. D., Jr. (1985) *Inorg. Chem. 24*, 895−900.
54. Choppin, G. R., and Wang, Z. M. (1997) *Inorg. Chem. 36*, 249−252.
55. Ofelt, G. S. (1963) *J. Chem. Phys. 38*, 2171−2180.
56. Cate, J. H., Hanna, R. L., and Doudna, J. A. (1997) *Nat. Struct. Biol. 4*, 553−558.
57. Agris, P. F., Stuart, J. W., Guenther, R., and Basti, M. M. (1996) *Magn. Reson. Chem. 34*, S87−S96.
58. Yue, D., Kintanar, A., and Horowitz, J. (1994) *Biochemistry 33*, 8905−8911.
59. Kowalak, J. A., Dalluge, J. J., McCloskey, J. A., and Stetter, K. O. (1994) *Biochemistry 33*, 7869−7876.
60. Hingerty, B. E., Brown, R. S., and Jack, A. (1978) *J. Mol. Biol. 124*, 523−534.
61. Holbrook, S. R., Sussman, J. L., Warrant, R. W., and Kim, S. (1978) *J. Mol. Biol. 123*, 631−660.
62. Wu, S. L., and Horrocks, W. D., Jr. (1996) *Anal. Chem. 68*, 394−401.
63. Jucker, F. M., Heus, H. A., Yip, F. P., and Moors, E. H. M. (1996) *J. Mol. Biol. 264*, 968−980.
64. Hansen, M. R., Simorre, J.-P., Hanson, P., Mokler, V., Bellon, L., Beigelman, L., and Pardi, A. (1999) *RNA 5*, 1099−1104.
65. Horton, T. E., Clardy, D. R., and DeRose, V. J. (1998) *Biochemistry 37*, 18094−18101.
66. Beeby, A., Clarkson, I. M., Dickins, R. S., Faulkner, S., Parker, D., Royle, L., de Sousa, A. S., Williams, J. A. G., and Woods, M. (1999) *J. Chem. Soc., Perkin Trans. 2*, 493−503.
67. Catalán, J., Del Valle, J. C., Díaz, C., Palomar, J., De Paz, J. L. G., and Kasha, M. (1999) *Int. J. Quantum Chem. 72*, 421−438.
68. Misra, V. K., and Draper, D. E. (2000) *J. Mol. Biol. 299*, 813−825.

BI002210U